Supplementary Material

Halopseudomonas species: cultivation and molecular genetic tools

Luzie Kruse[1], Anita Loeschcke[1], Jan de Witt[2], Nick Wierckx[2], Karl-Erich Jaeger[1,2*], Stephan Thies[1*]

[1]Institute of Molecular Enzyme Technology, Heinrich Heine University, Düsseldorf, Germany
[2]Institute of Bio- and Geosciences IBG-1: Biotechnology, Forschungszentrum Jülich, Germany

Correspondence: Name (e-mail): Stephan Thies (s.thies@fz-juelich.de)
Karl-Erich Jaeger (k.-e-jaeger@fz-juelich.de)

Supplementary Methods

Bacterial strains and plasmids

All bacterial strains, plasmids and oligonucleotides that were used in this study are listed in

Table S1: Bacterial strains, plasmids and oligonucleotides used in this study.

strain / plasmid / sequence	features, sequences	references
	bacterial strains	
E. coli DH5α	*F- φ80lacZΔM15 Δ(lacZYA-argF)U169 recA1 endA1 hsdR17 phoA supE44 thi-1 gyrA96 relA1 deoR*	Hanahan, 1983
E. coli DH5α λpir	λpir phage lysogen of DH5α	Penfold and Pemberton, 1992
E. coli S17-1	*Ec294::*[RP4-2(Tc^R::Mu)(Km^R::Tn7)]*recA, thi, pro, hsdR- hsdM+* TP^R, Sm^{R+}	Simon et al., 1983
E. coli S17.-1λpir	λpir phage lysogen of S17-1	Simon et al., 1983
Stellar™ chemically competent cells	*F–, endA1, supE44, thi-1, recA1, relA1, gyrA96, phoA, Φ80d lacZΔ M15, Δ(lacZYA - argF) U169, Δ(mrr - hsdRMS - mcrBC), ΔmcrA, λ–*	Takara Bio Inc, Japan
H. aestusnigri VGXO14	wilde-type	Sánchez et al., 2014
H. bauzanensis BZ93	wild-type	Zhang et al., 2011
H. litoralis 2SM5	wild-type	Pascual et al., 2012
H. oceani KX20	wild-type	Wang and Sun, 2016
H. aestusnigri VGXO14R	wild-type, spontaneous Rif^R-variant	this study
H. bauzanensis BZ93R	wild-type, spontaneous Rif^R-variant	this study
H. litoralis 2SM5R	wild-type, spontaneous Rif^R-variant	this study
H. oceani KX20R	wild-type, spontaneous Rif^R-variant	this study
H. litoralis Tn7-P$_{em7}$-*msfgfp*	Rif^R, Tn7: P$_{em7}$, *msfgfp*, Gm^R	this study
H. litoralis Tn7-P$_{tac/lacI}$-*mcherry*	Rif^R, Tn7: *lacI*, P*tacI*, *msfgfp*, Km^R	this study
H. litoralis Tn7.1-P$_{tac/lacI}$-*mcherry* Tn7.2-P$_{em7}$-*msfgfp*	Rif^R, Tn7.1: *lacI*, P*tacI*, *msfgfp*, Km^R; Tn7.2: P$_{em7}$, *msfgfp*, Gm^R	this study
	plasmids	
pBG13	Km^R, Gm^R, *ori R6K*, pBG-derived, P$_{em7}$	Zobel et al., 2015
pBNT-*mcherry*	pBBR1-MCS-derivative, Km^R, P$_{nagAa/nagR}$, with EcoRI/XbaI inserted *mcherry*	Hogenkamp et al., 2021
pBTBX-2-mcs	pBBR1-MCS2-derivative, Km^R, P$_{araBAD/araC}$, mcs	Prior et al., 2010
pBTBX-*sfgfp*	pBBR1-MCS2-derivative, Km^R, P$_{araBAD/araC}$, with InFusion inserted *sfgfp*	this study
pJT'Tmcs	Amp^R, Gm^R, P$_{tac}$, mcs, non-mobilisable	Verhoef et al., 2010
pJT'Tmcs-*mcherry*	Amp^R, Gm^R, P$_{tac}$, *mcherry*, non-mobilisable	Burmeister et al., 2019
pTNS2	pUC18R6KT-derivative with EcoRI/ClaI inserted P$_{lac}$-*tnasABCD*	Choi et al., 2005
pUC18R6KT-miniTn7T-Km	pUC18R6KT-miniTn7T-derivative, Amp^R, Km^R	Choi et al., 2005
pUC18R6KT-miniTn7T-Km-P$_{tac/lacI}$-*mcherry*	pUC18R6KT-miniTn7T-derivative, Amp^R, Km^R, *lacI,* P$_{tac}$-*mcherry*	this study

strain / plasmid / sequence	features, sequences	references
pVLT33-GFPmut3	pVLT33-derivative, Km^R, *lacIq*, P_{tac}*gfpmut3*	Hogenkamp et al., 2021
pYT-P_{em7}-*eYFP*	pYT-derivative, Km^R, Gm^R, P_{em7}, *eyfp*	Weihmann et al., 2023; A. Sieberichs, unpublished
pHT01-sfGFP	pHT01-derivative, Cm^R, Amp^R, *lacI*, P_{grac}-*sfgfp*	Hogenkamp et al., 2021
	oligonucleotides	
(1) IF_sfGFP_pBTBX_fw	binds at the 5'end of the *sfgfp* gene on pHT01-sfGFP, inserts homologous region for InFusion® cloning. 5'-GATATACCCATGGGCATGAGCAAAGGAGAAGAACTTTTCACTG	this study
(2) IF_sfGFP_pBTBX_rev	binds at the 3'end of the *sfgfp* gene on pHT01-sfGFP, inserts homologous region for InFusion® cloning. 5'-TTCGTTGACGAATTTTCATTTGTAGAGCTCATCCATG	this study
(3) pBTBX_fw	binds at the 3'end of the plasmid pBTBX-2-mcs downstream MCS, inserts homologous region for InFusion® cloning. 5'-GTTCTAGAAAATTCGTCAACGAATTCAAGCT	this study
(4) pBTBX_rev	binds at the 5'end of the plasmid pBTBX-2-mcs upstream MCS, inserts homologous region for InFusion® cloning. 5'-GCCCATGGGTATATCTCCTTCTTAAAG	this study
(5) IF_Ptac_pUC18R6K_fw	binds at the 5'end of *lacI* P_{tac} region on pVLT33, inserts homologous region for InFusion® cloning and KpnI site for further exchanges. 5'-GCCTGCAAGGCCTTCGCGAGGTACCTCACTGC CCGCTTTCCAGTCGG	this study
(6) IF_Ptac_pUC18R6K_rev	binds at the 3'end of *lacI* P_{tac} region on pVLT33, inserts homologous region for InFusion® cloning and KpnI site for further exchanges. 5'-TCGAGAAGCTTGGGCCCGGTACCAATTGTTATCCGCTCACAATTCCAC	this study
(7) IF_RBS-mCherry-mTn7_fw	binds at the 5'end of *mcherry* gene on pJT'Tmcs, inserts homologous region for InFusion®. 5'-ACCGGGCCCAAGCTTCTCGATTCACACAGGAAACAGGAGGTACC	this study
(8) IF_RBS-mCherry-mTn7_rev	binds at the 3'end of *mcherry* gene on pJT'Tmcs, inserts homologous region for InFusion®. 5'-GGGCTGCAGGAATTCCTCGATTACTTGTACAGCTCGTCCATGCCG	this study
(9) attTn7_pBG13_fw	binds within *msfgfp* gene for proving genetic integration. 5'-CCGATCCTGGTTGAACTGGATG	this study
(10) attTn7_pUC_fw	binds within *Km^R* gene for proving genetic integration. 5'- CAGGACATAGCGTTGGCTAC	this study
(11) pTn7R_fw	binds within the Tn7R recognition site. 5'-CACAGCATAACTGGACTGATTTC	Choi and Schweizer, 2006
(12) 2SM5_glmS1_rev	binds specifically in *glmS*1 gene of *H. litoralis* 2SM5 (*BLU11_RS05420*) for proving genetic integration. 5'-TCAAGCATGGGCCATTGGCG	this study

strain / plasmid / sequence	features, sequences	references
(13) 2SM5_glmS2_rev	binds specifically in *glmS*1 gene of *H. litoralis* 2SM5 (*BLU11_RS05420*) for proving genetic integration. 5'- AACATGGCCCTCTGGCACTG	this study

Recombinant DNA techniques were applied as described by Sambrook et al. (1989) using DH5α, or in the case of an expression vector harbouring an *oriR6K*, DH5α λpir was used. The construction of expression vectors was either carried out via restriction and ligation cloning or InFusion® Cloning (Takara Bio Europe, St Germain en Laye, France). For pBTBX-sfGFP, the insert was generated by amplifying the *sfgfp* gene on pHT01-sfGFP with oligos 1 and 2. The plasmid pBTBX-2-mcs, a gift from Ryan Gill (Addgene plasmid # 26068), was amplified using oligos 3 and 4. PCR fragments were assembled via InFusion® Cloning (Takara Bio Europe, St Germain en Laye, France). pUC18R6KT-miniTn7T-Km-Ptac/lacI-mCherry was constructed by first amplifying the *lacI*-P_{tac} fragment encoded on pVLT33 using oligos 5 and 6. The pUC18R6KT-miniTn7T-Km vector, which was a gift from Herbert Schweizer (Addgene plasmid # 64969; http://n2t.net/addgene:64969; RRID: Addgene_64969) was linearised via restriction with KpnI. Thus, the two fragments were assembled using InFusion® Cloning (Takara Bio Europe, St Germain en Laye, France). In a second step, the *mcherry* sequence, including the P_{tac} RBS, was amplified using oligos 7 and 8 and was assembled with XhoI linearised pUC18R6KT-miniTn7T-Km-P_{tac} vector via InFusion® Cloning (Takara Bio Europe, St Germain en Laye, France).

***oriC* sequence *H. litoralis* 2SM5**

location of *oriC in* : LT629748.1: 3507165 – 3507739 nt (575 nt)

CTTCAGATACCTGAGTAATTCACGACAGAGCCGCTAAGCCCTTTCAAGGGATCGGGAAT
TCTAGAGAAGAAGCGGGCTCAGGTCAATTTGAATTCTCAGTAGGTAGATAAATAACAATA
CAAAGAAAAGATTTTTAAAAGATTATGTATGTAGATCTTAATGAGGAAGGGATTTTCTGTG
GATAAGGGGGCCCACGCCAGATAGGCCGCTCGATTGCCGAGAGCACAACTCGGTGAG
TAAATTGTTCACAGAGGGCATCATCCATTGTGCAGCCCCTGTGGATAACAGGTCTTGAT
ATCCACAGGGGGATTTATCCCCTGTTTTCACTCCCGTTTGCCAACAGACTGATACAGAC

CTTGTCCACAAGGCTCATGCTGCCGGTTTTACAAGGACGAGCGCTGATAAATGCAACGT
AATTCAGGCGCAAGAGCCTCGGGCGATCCTATCTGTGATGTGGATAAGTAAGGGGGGA
AAGGCTAGAATGACGGGTGTTTCCCCGGGGCTGACGAGTGCTGCTTCGGGGAAGGTTT
TTATCAACAACTCGAGCCGCTCAGGCTTGGAGTCGGGGGAATTCA

***oriC* sequences *B. mallei* ATCC23344**

location of *oriC in* : LT629748.1: 3,006,500-3,006,897 nt (398 nt)

ACCGCCCGCGGCCGGCGCACGCTCGCCATCCGGGCAATCGCACGACGCACCGCGAC
GGCGCTCGGCGATACGCGGAAGCGACATCCTCACAGATACGCCGGCCGGTTATCCAC
GTCACCCTGTGGATAACCGCGCAAATTCCCGACCCAATCGCTGTGCAACCGATGTGGA
CGTAAACGGGGTAACTCCGCACGGCCGCACAGACCCGAAAAAGTTGCCCATTGAAACC
CTGTGCGGGCAAACAGGCTGTGCGTCCGGTTATGCGCCCCGCAAGTGCATGATCCGG
CGGCGTAAACGCCGGTTATCCACAGAAAAACGGGTGTCTTGTTAACTCTTACTACGTAT
GTATACAGGTTTACCTCAAGATAAAGAGGCCTACCTCCACGATCGGCCACCGT

location of *oriC*: 3,055,348-3,055,787 nt (440 nt)

GCGCAAGCCCTTCGATGCTGCGGCGCGACGGGTCGAATTTGCGCAAACACGACTAAAC
AGGGCGTAAGCGCCCGTCCGATGGCACTCTTATGCTTGTCAAGACTTGACTTATGCACA
TTTTCCTCGTTGCAGCGCGGTAGAGGGCGGCATCGGCGAGCGGGCCGCGCTATGACG
GCGGAAATCGGATAGCAGCCTTGCCGGACAAGGCTTCCCGGGTTGCCCGCCCAATCG
GGAAAAAGCAGTGGGTGGCCGGATGCAGCGCCATTTCGCGGCCGTCAAGGGCGAGTT
CTCAACAAAGTTATCCACAGGATCGGCGAGCGCGCCGCGATTCTTAATGAGAATCCAAA
ACTTAGCGCCGAAAGTGACGTTTCACTTTAACTTCACGGGCGTCGCGGATATCCGGCCT
GCCGGGCCTGTCGGCATTCGGCGGTGCCGCACCG

Supplementary Data

Growth of *Halpseudomonas* spp. under typical laboratory conditions

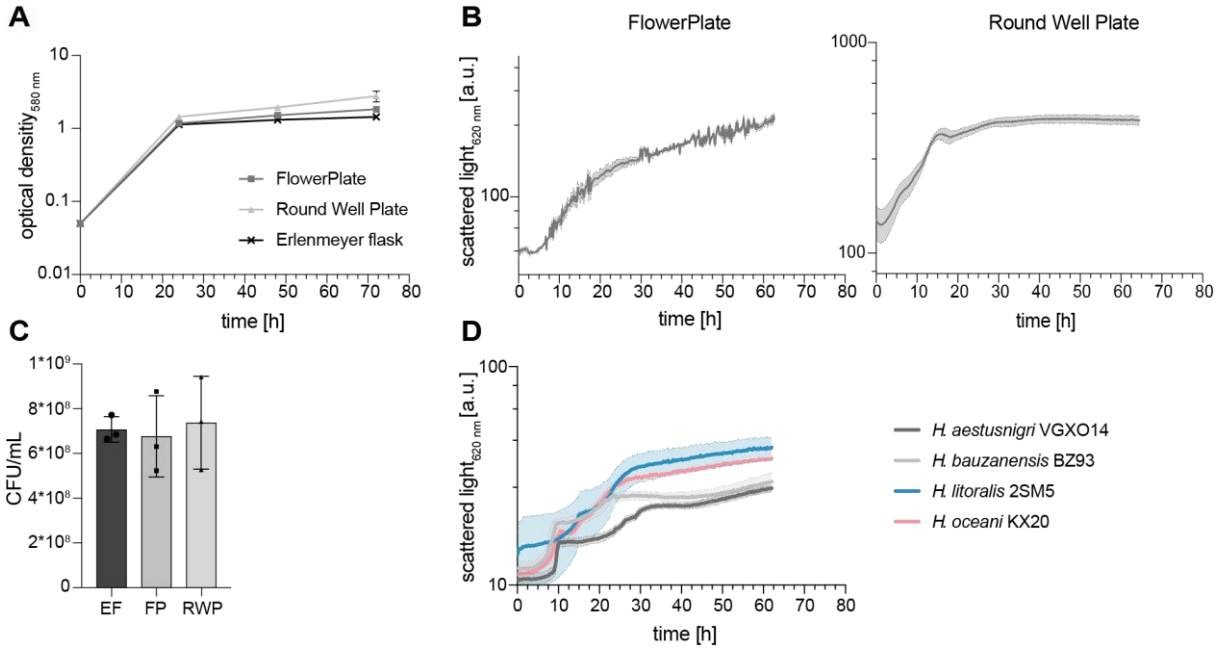

Figure S1: Elucidation of different cultivation vessels on bacterial growth.
A+C: Shown is exemplarily the growth of *H. bauzanensis* BZ93 when cultivated in LB-Medium at 30 °C and 130 rpm in an Erlenmeyer flask (EF, black cross), 1000 rpm in a Flower Plate® (FP, dark grey square) or Round Well Plate® (RWP, light grey triangle). **A:** Samples of each culture were taken every 24 h for 72 h to determine the optical density at 580 nm. **B:** Main cultures were inoculated with the same pre-cultures and then cultivated in different BioLector I systems to compare the growth behaviour using an FP or RWP. **C:** After 24 h of cultivation, samples were taken from each cultivation vessel and plated on agar plates for CFU measurements. **D:** Growth of *H. aestusnigri* VGXO14, *H. bauzanensis* BZ93, *H. litoralis* 2SM5, and *H. oceani* KX20 cultivated in LB medium in Round Well Plates. The shown data represent the mean of biological triplicates. The calculated standard deviations are either indicated by shadows or error bars

The optical density and the CFU measurements showed no differences in using different cultivation vessels. The growth curves showed differences instead. Application of FlowerPlates® led to jagged growth curves and aggregate formation within the cultures, whereas the aggregate formation was reduced and the growth curve smoother when using a Round Well Plate®. The differences in the arbitrary units as a measure for light scattering are due to the use of different BioLector devices. The biomass (scattered light intensity) at 620 nm at gain 30 is shown in both cases. That there are no differences in living cells is proven by CFU measurements. Multiphasic growth can be observed within all Halopseudomonads indicating a subsequent metabolism of complex media carbon sources and therewith the need for further improvement.

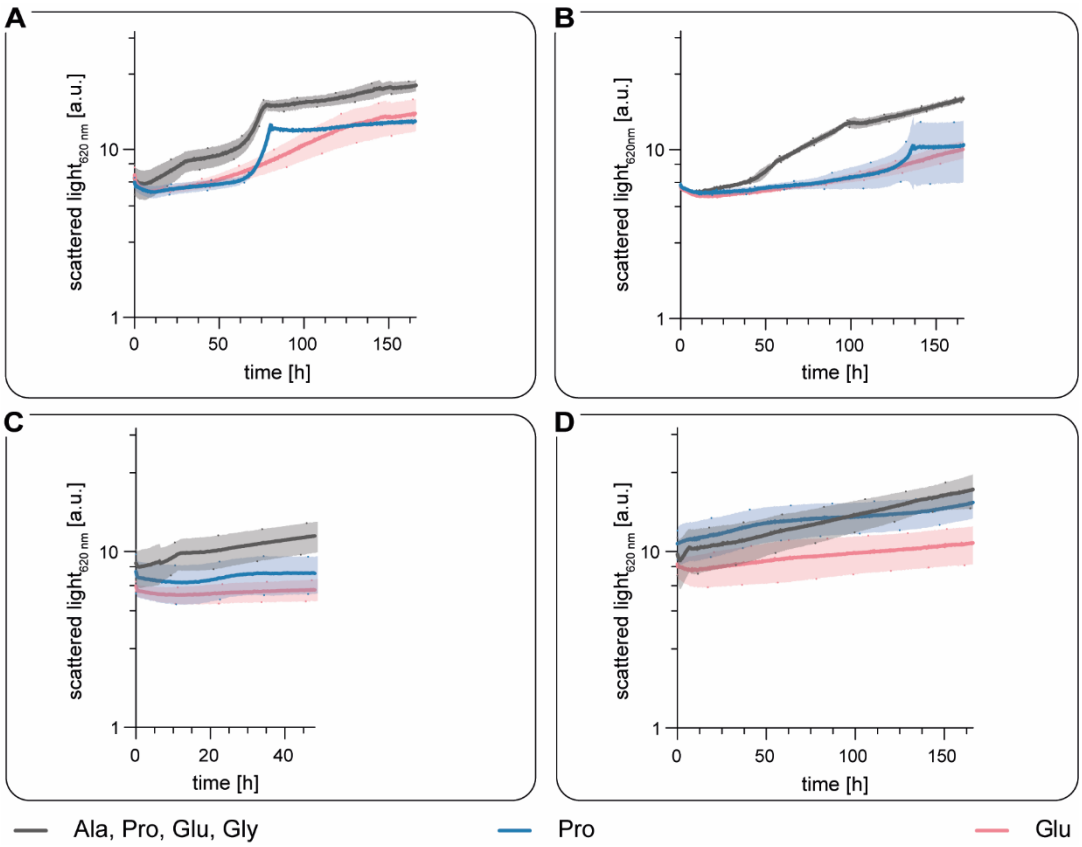

Figure S2: Multiphasic growth on a defined amino acid cocktail.
H. aestusnigri VGXO14R (**A**), *H. bauzanensis* BZ93R (**B**), *H. litoralis* 2SM5R (**C**), and *H. oceani* KX20R (**D**) from pre-cultures grown in LB medium were cultivated in Round Well Plates® in HM medium supplemented with a mixture of the amino acids DL-alanine, L-proline, L-glutamine, and glycine (dark grey), with L-proline (blue), or L-glutamine (red), as single carbon source. The shown data represent the mean of a biological duplicate or triplicate. Cultivation was pursued until all cultures of a species achieved the stationary phase, or maximal 160 h. The calculated standard deviations are indicated by shadows.

DL-alanine, L-proline and L-glutamine were deduced from the carbon source utilisation profiles (Figure S4) as suitable carbon sources to create model amino acid mix mimicking the major component cocktail of LB broth accessable for the growth of the *Halopseudomonas* species; glycine, which was not part of the carbon profiling, was addionally selected. All amino acids were applied in C-eqimolar conncentrations to 0.6 g/L DL-alanine. Cultures on single amino acids showed monophasic growth behaviour, whereas the mixture led to multiphasic growth; thus indicating, a subsequent metabolism of the available carbon sources. Notably, non of the investigated strains was able to metabolise glycin (not shown).

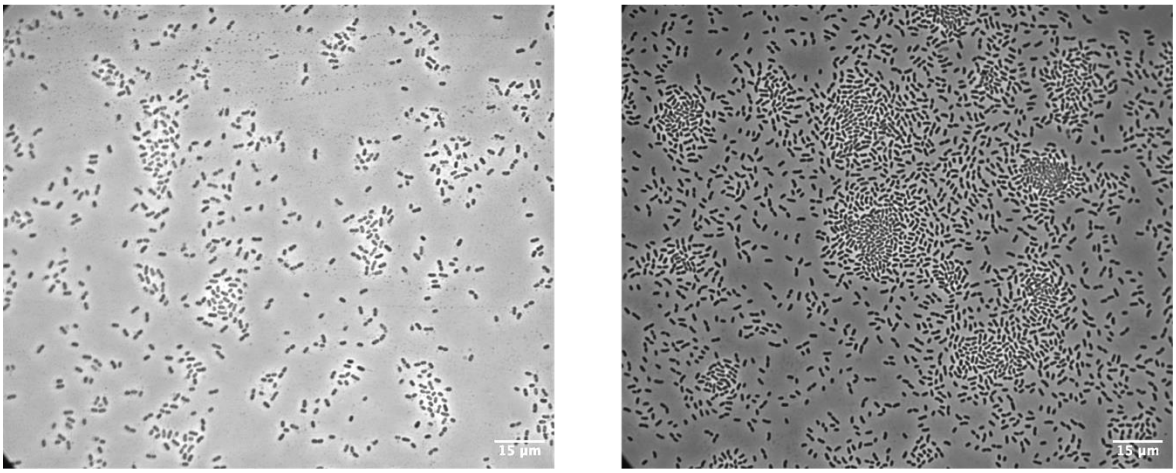

Figure S3: Phase contrast microscopy images of *H. litoralis* 2SM5 (left) and *H. oceani* KX20 (right).
A zoom-in of these pictures is shown in Figure 1. The images were taken of motile bacteria from stationary phase culturesshwoing tendency to aggregate**.** A scale bar of 15 µM is shown.

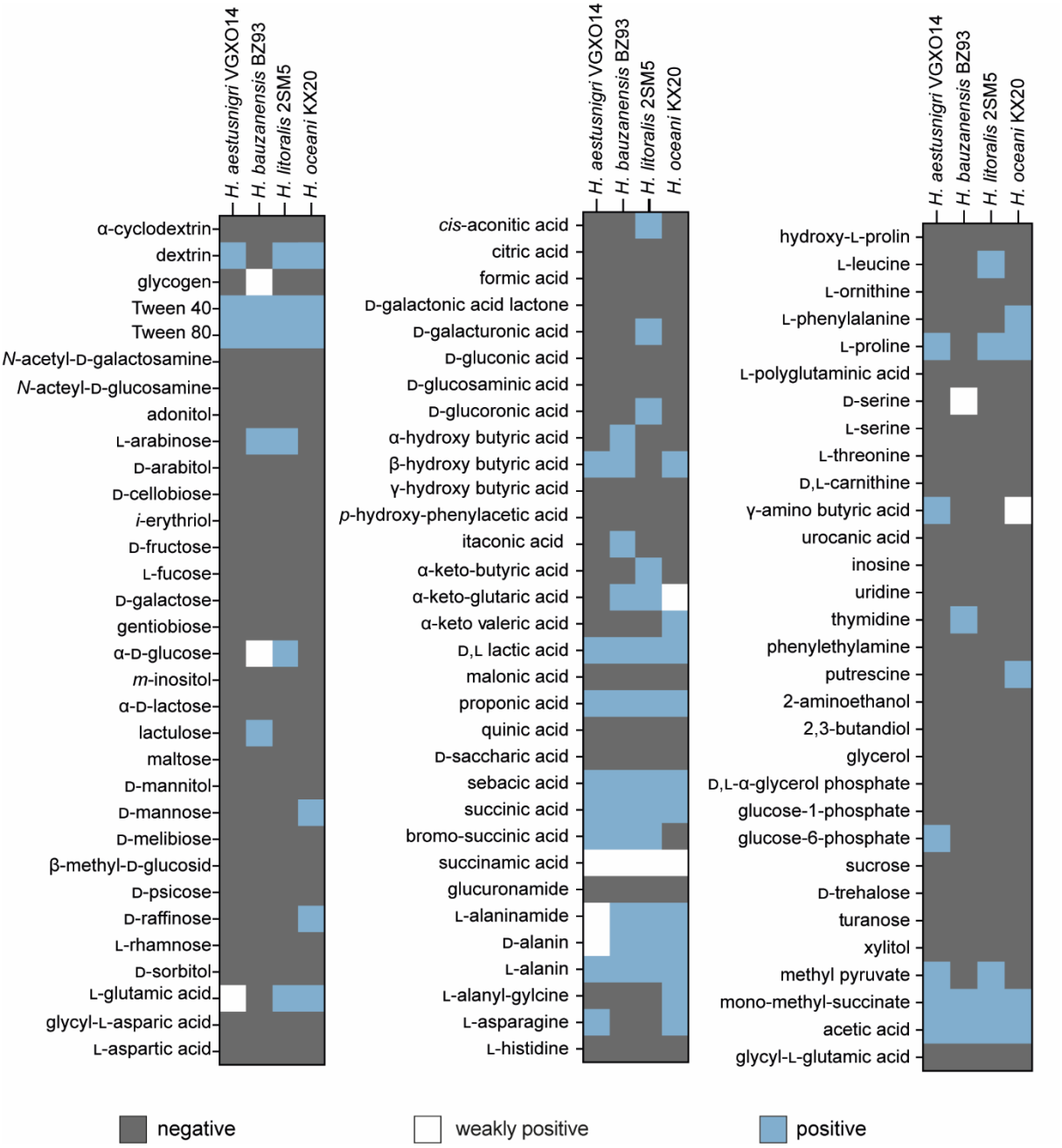

Figure S4: Carbon source utilisation profiles of *H. aestusnigri* VGXO14, *H. bauzanensis* BZ93, *H. litoralis* 2SM5 and *H. oceani* KX20 according to previous studies.
The data shown represents a summary of the carbon sources that can be ustilized by the four *Halopseudomonas* species, according to the information from the respective strain type descriptions. The profiles were determined using API (Analytical Profile Index) 20 tests or Biolog phenotyping microplates. (Zhang *et al.*, 2011; Pascual *et al.*, 2012; Sánchez *et al.*, 2014; Wang and Sun, 2016). The terminology to categorize growth strength (“negative”, “weakly positive”, “positive”) is given as stated in the respective original publications. In the present study, the spectrum is extended by showing growth on malonic acid, glutaric acid, pimelic acid, azelaic acid, adipic acid and suberic acid (table 1).

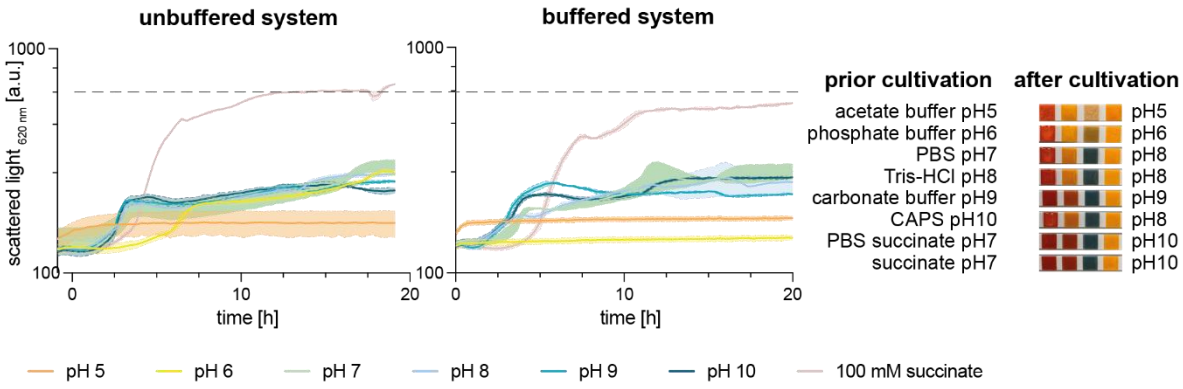

Figure S5: Determination of the effect of pH on bacterial growth.
H. litoralis 2SM5 was cultivated in LB medium adjusted to pH values from 5 – 10. In one experimental setup, unbuffered systems were used; in another, buffered systems with 100 mM of buffer component. In the latter, acetate buffer was used to adjust pH5, phosphate buffer for pH6, PBS for pH7, Tris-HCl for pH8, carbonate buffer for pH9, and CAPS for pH10. For comparison, 100 mM succinic acid supplementation was tested with (PBS, pH7) and without buffer. The shown data represent the mean of a biological triplicate. Shadows indicate the calculated standard deviation. The adjusted pH values before and after the cultivation are shown on the right hand. The displayed data represent the mean of a biological triplicate. Shadows indicate the calculated standard deviation.

The comparison of *H. litoralis* cultivated in an unbuffered and buffered LB-Medium showed that the bacteria did not grow faster at basic pH values. Thus, growth improvement could be tracked down to the addition of the succinic acid improved the growth behaviour, even though the buffer capacity of 100 mM was still not suitable to keep a steady pH.

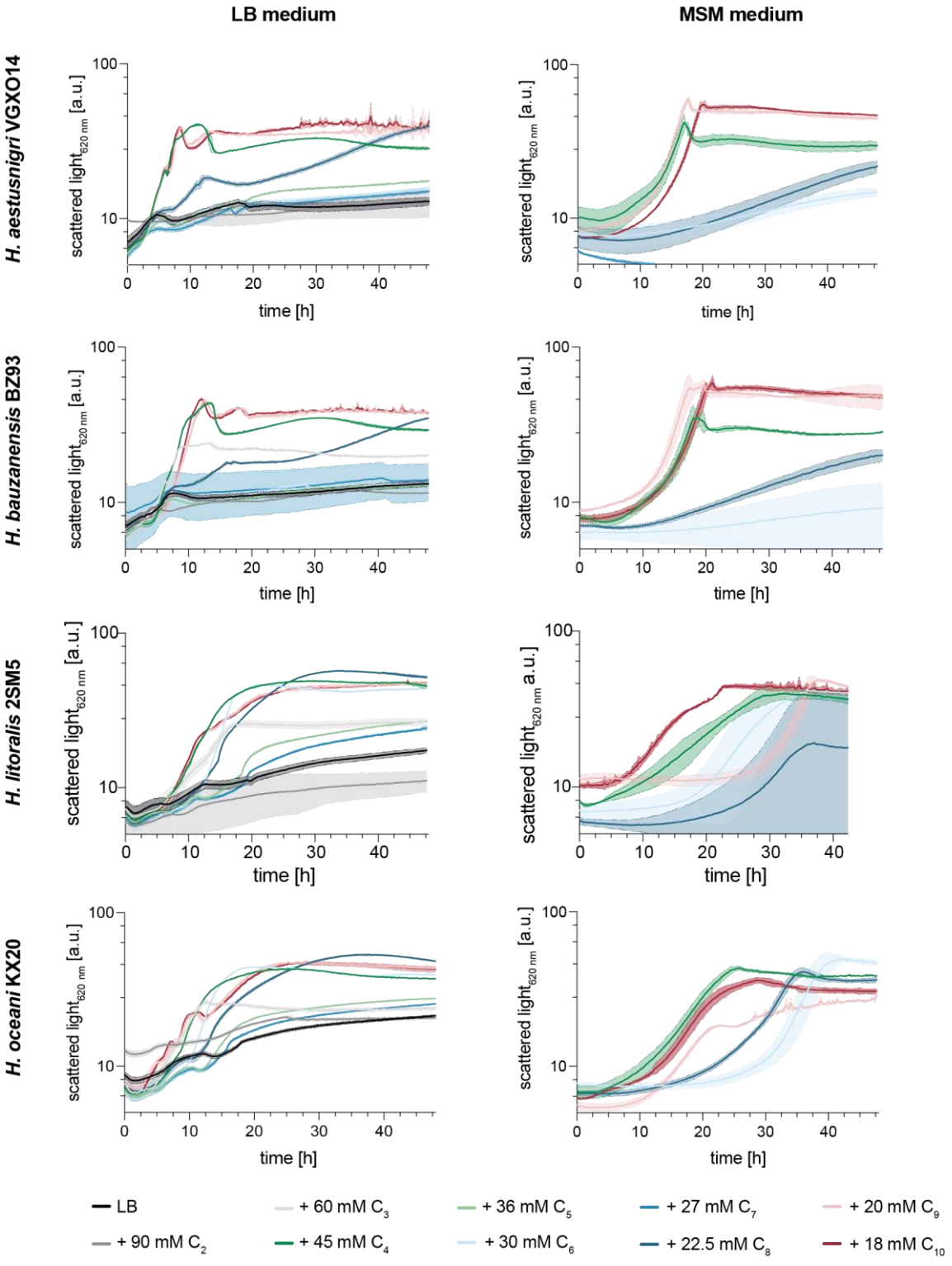

Figure S6: Growth curves of *H. aestusnigri* VGXO14, *H. bauzanensis* BZ93, *H. litoralis* 2SM5, and *H. ocenai* KX20 summarised in Table 1.
The C_2 – C_{10} dicarboxylic acids were tested in C-equimolar concentrations to 45 mM succinic acid and were used as an additional carbon source in LB medium and as sole carbon sources in MSM medium. The shown data represent the mean of a biological triplicate. Shadows indicate the calculated standard deviation.

Table S2: Homologue proteins to enzymes described for dicarboxylic acid degradation in *A. baylyi* ADP1.

*,** identical protein

Protein	*H. aestusnigri* Locus-tag	% ident	*H. bauzanensis* Locus-tag	% ident	*H. litoralis* Locus-tag	% ident	*H. oceani* Locus-tag	% ident
DcaK	B7O88_RS06080	19	BMY02_RS03645*	26	BLU11_RS07280**	24		
DcaP			WP_218144722.1	22				
MucK	WP_200818422.1	24	BMY02_RS03645*	29	BLU11_RS07280**	24	C1949_RS05600	21
DcaI	B7O88_RS07895	25	BMY02_RS10000	47	BLU11_RS15730	48		
DcaJ			BMY02_RS10005	47	BLU11_RS15510	47		
DcaA	B7O88_RS16455	35	BMY02_RS10200	79	BLU11_RS06175	80	C1949_RS01775	35
DcaE	B7O88_RS01040	39	BMY02_RS13030	44	BLU11_RS12290	42	C1949_RS02560	39
DcaH	B7O88_RS11070	47	BMY02_RS16220	48	BLU11_RS15865	47	C1949_RS00785	47
DcaF	B7O88_RS11065	68	BMY02_RS16215	66	BLU11_RS15870	66	C1949_RS00790	68

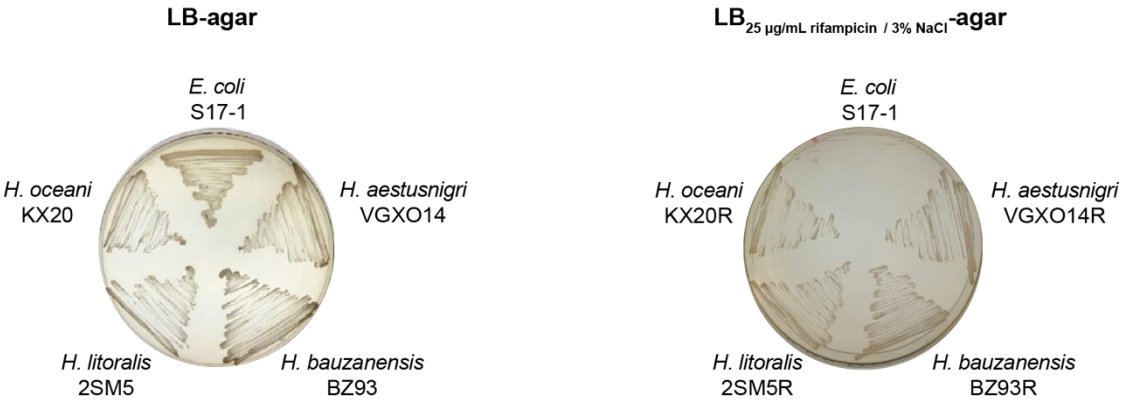

Figure S7: Isolation of Rif^R Strains.
Growth of *H. aestusnigri* VGXO14R, *H. bauzanensis* BZ93R, *H. litoralis* 2SM5R, *H. oceani* KX20R, and *E. coli* S17-1 on LB-agar and LB agar containing 25 µg/mL Rif and 3% (*w/v*) NaCl.

Several colonies of each species were plated on LB-agar containing 25 µg/mL rifampicin (Rif); grown colonies were plated again to confirm rifampicin resistance. The resulting strains were termed *H. aestusnigri* VGXO14R, *H. bauzanensis* BZ93R, *H. litoralis* 2SM5R, and *H. oceani* KX20R, respectively. To counteract spontaneously occurring Rif-resistant cells of the *E. coli*-donor strain, we exploited the pronounced osmotolerance of *Halopseudomonas spp.* by using LB agar plates containing Rif and 3% (*w/v*) NaCl, which impaired the donor's growth.

Table S3: Replicability of different origins of replication in selected *Halopseudomonas* strains.
The replicability of an *oriV* is indicated by +. Non-replicable *oriVs* are indicated by -.

oriV	Plasmid backbone	*H. aestusnigri*	*H. bauzanensis*	*H. litoralis*	*H. oceani*
RO1600	pJT'Tmcs	+	+	+	+
RSF1010	pVLT33	+	+	+	+
pBBR1	pBTBX-2-mcs	+	+	+	+
pMB1	pYT	+	+	+	+
R6K	pUC18R6KT	-	-	-	-

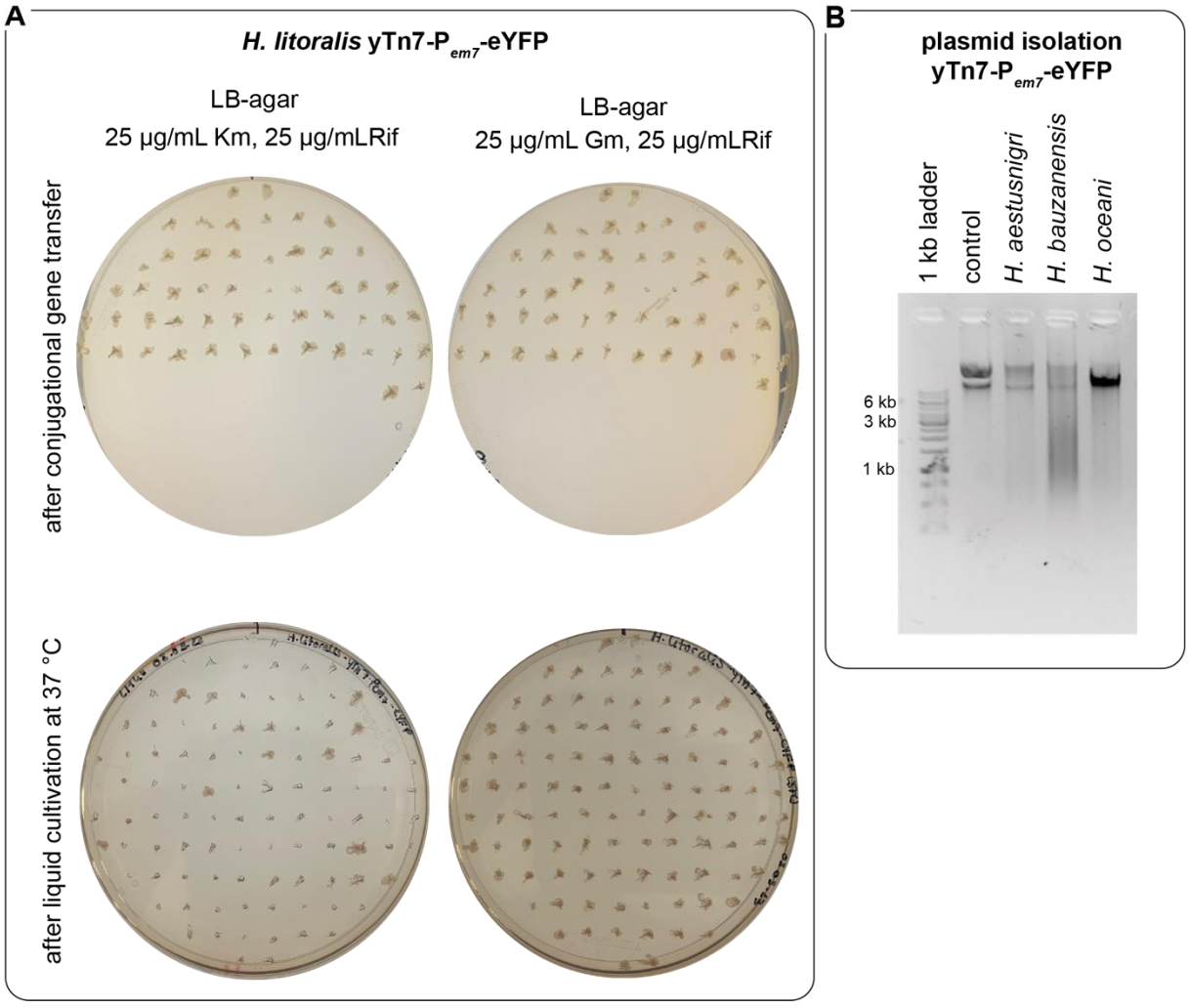

Figure S8: Conjugational transfer, transposition and plasmid curing of *H. litoralis* 2SM5R using the pMB1 plasmid yTREX-Tn7-P$_{em7}$-eYFP.
A: The upper row shows the selection plates for *H. litoralis* yTREX-Tn7-P$_{em7}$-eYFP on LB-agar containing the antibiotics rifampicin and kanamycin (vector backbone marker) and rifampicin and gentamycin (transposon marker), respectively. The second row shows colonies grown on the same selection plates after a heat stress treatment, incubating at 37 °C for 24 h. **B:** The isolated plasmids of yTn7-P$_{em7}$-eYFP from cultures of *H. aestusnigri*, *H. bauzanensis,* and *H. litoralis* grown in the presence of kanamycin after the transformation with the respective plasmid are shown. Control: yTn7-P$_{em7}$-eYFP isolated from *E. coli*

The plasmid yTREX-Tn7-P$_{em7}$-eYFP harbours a pMB1 origin of replication typically replicated in *E. coli*. *H. litoralis* transformed with this plasmid is resistant towards kanamycin and gentamycin, which resistance-conferring genes are encoded in the backbone and integration cassette, respectively, thus, indicating that the plasmid was maintained. This was confirmed by the isolation of this plasmid (**Figure S8B**). Cultivation in LB medium under gentamycin selection pressure at 37 °C for 24 h induced this transposition, which can be seen by the loss of kanamycin resistance and was also confirmed via sequencing analysis.

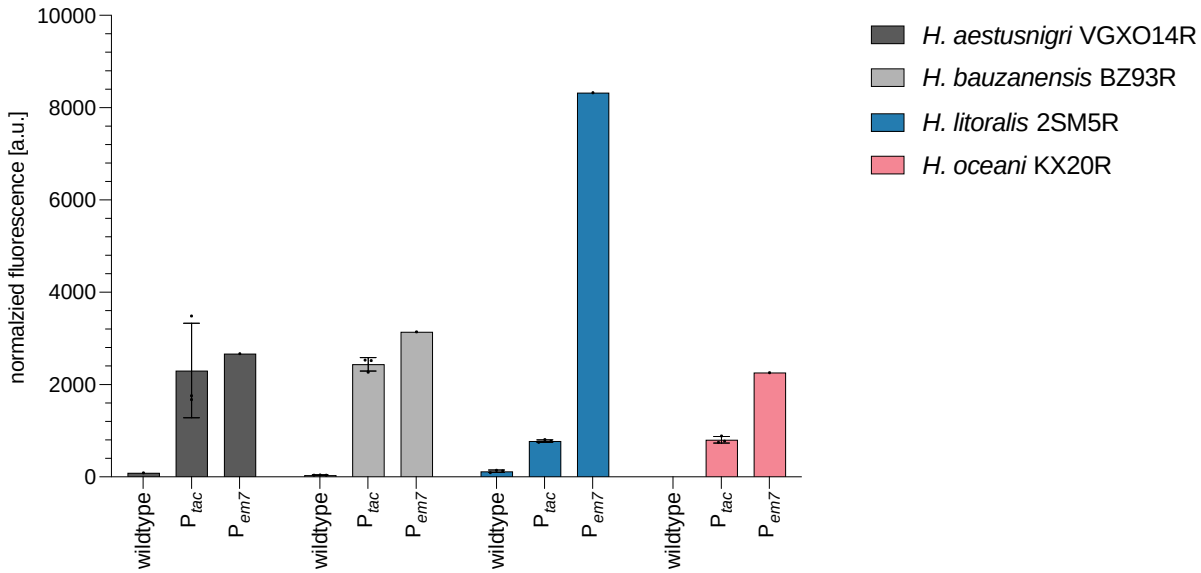

Figure S9: Normalised fluorescence signals of *H. aestusnigri* VGXO14R, *H. bauzanensis* BZ93R, *H. litoralis* 2SM5R, and *H. oceani* KX20R harbouring constitutive expression systems.
The used plasmids were pJT'Tmcs-*mcherry* (P_{tac}) and pYT-P_{em7}-*eYFP* (P_{em7}). Shown here is the normalised fluorescence intensity of one sample out of a biological triplicate (P_{em7}) and the mean and standard deviation of a biological triplicate (P_{tac}) after 24 h of cultivation.

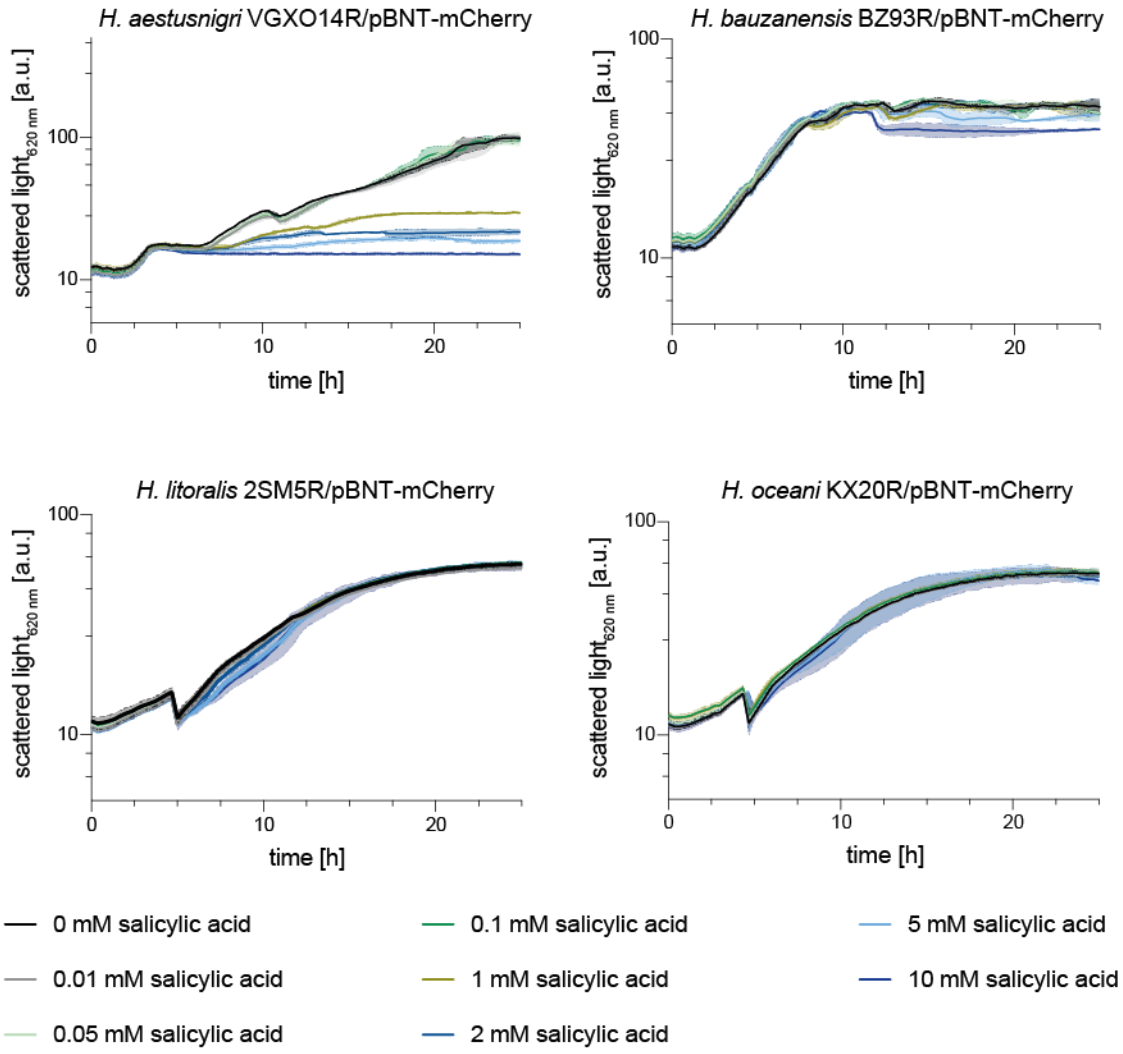

Figure S10: Growth curves of *H. aestusnigri* VGXO14R, *H. bauzanensis* BZ93R, *H. litoralis* 2SM5R, and *H. oceani* KX20R harbouring pBNT-mCherry with different concentrations of salicylic acid.
Increasing concentrations of the inducer salicylic acid (0 – 10 mM) were added to the cultures after 4.5 h of cultivation. The bacterial growth was monitored using the BioLector I system. 0 mM salicylic acid: black; 0.01 mM salicylic acid: grey; 0.05 mM salicylic acid: pale green; 0.1 mM salicylic acid: green; 1 mM salicylic acid: olive; 2 mM salicylic acid: blue; 5 mM salicylic acid: light blue; 10 mM salicylic acid: dark blue. The shown data represent the mean of a biological triplicate. Shadows indicate the calculated standard deviation.

Chromosomal integration of reporter genes by Tn7 transposition

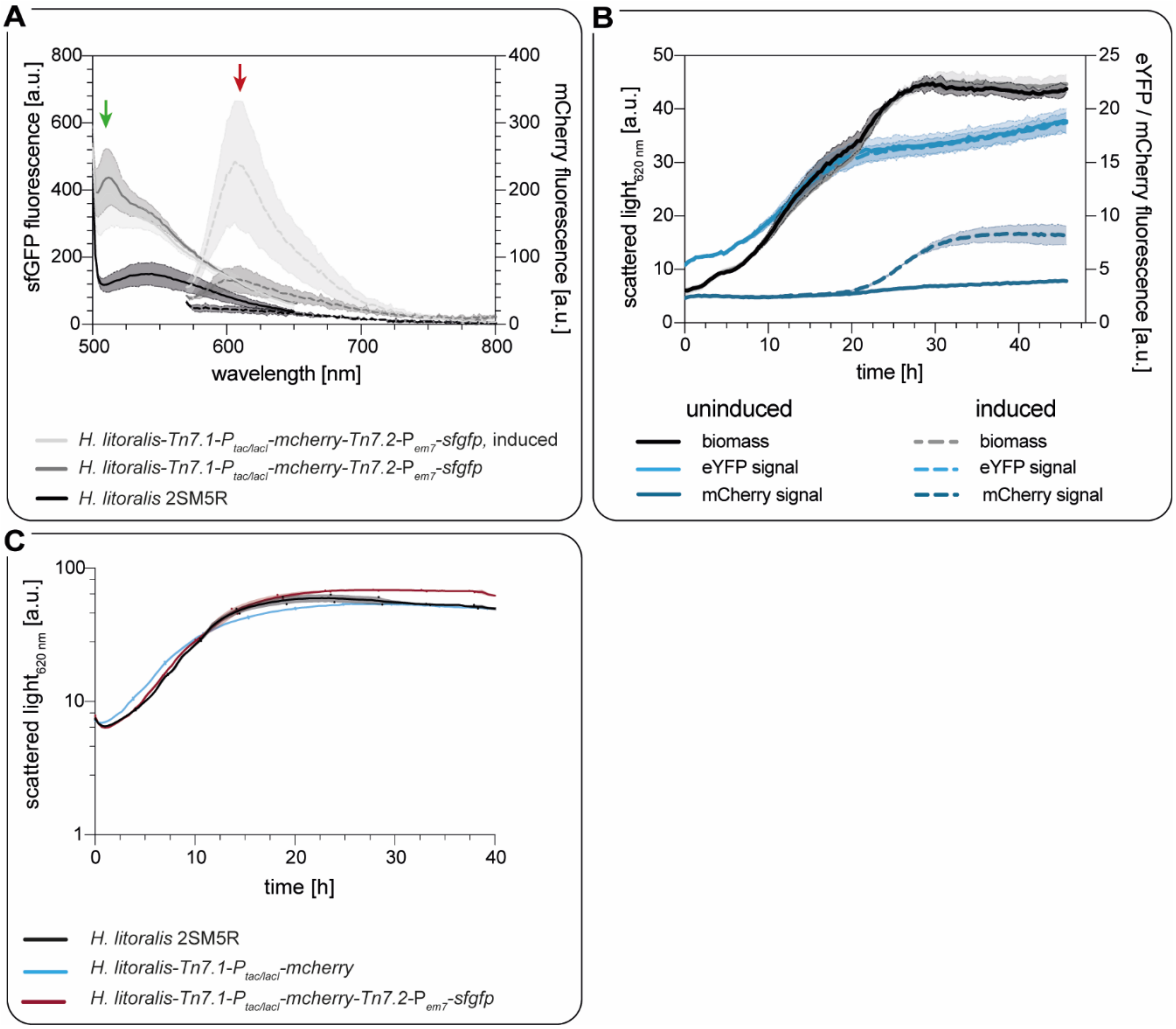

Figure S11: Emission spectra and growth profiles of three *H. litoralis* 2SM5R yTn7.1-P*em7*-sfGFP-P*tac/lacI*-mCherry after induction of *mcherry* gene expression.
A: sfGFP (continuous line, green arrow) and mCherry (dotted line, red arrow) emission spectra of *H. litoralis* Tn7.1-P*em7*-*sfgfp*-Tn7.2-P*tac*-*mcherry* after the induction with IPTG (light grey), the control (dark grey) and wild type as control (black). **B:** The biomass of *H. litoralis* (black, continuous line) as well as *H. litoralis* Tn7.1-P*em7*-*sfgfp*-Tn7.2-P*tac*-*mcherry* (grey, dotted line), as well as the sfGFP fluorescence (light blue, Tn7.1-site) and the mCherry fluorescence (dark blue, Tn7.2-site), were measured with a microbioreactor system (BioLector I). The cultures were induced with 50 µM IPTG (+, dashed line) after 4.5 h of cultivation. The respective dotted line shows the wild-type controls. **C:** Growth comparison of the cultures of *H. litoralis* supplemented with 50 µM IPTG shown in Figure 4C, D without (black) or with one (blue), and two (red) *att*Tn7-sites occupied. The data represent the mean of biological triplicates, and error bars or shadows indicate the calculated standard deviation.

The experimental setup in Figure S11B was the same as for the data shown in Figure 4 (main part). However, for 4 of 45 clones in this repeated experiment, the behaviour shown here was observed. The supplementation of IPTG leads to an induction of *mcherry* gene expression only 16 h after induction. In contrast, the GFP signal correlates with the biomass signal, as to be expected from a constitutively expressed gene, which was not observed in the other cultures (exemplarily shown in **Figure 4**, main part).

Supplementary References

Burmeister, A., Hilgers, F., Langner, A., Westerwalbesloh, C., Kerkhoff, Y., Tenhaef, N., et al. (2019) A microfluidic co-cultivation platform to investigate microbial interactions at defined microenvironments. *Lab Chip* **19**: 98–110.

Choi, K.H., Gaynor, J.B., White, K.G., Lopez, C., Bosio, C.M., Karkhoff-Schweizer, R.A.R., and Schweizer, H.P. (2005) A Tn7-based broad-range bacterial cloning and expression system. *Nat Methods* **2**: 443–448.

Choi, K.H. and Schweizer, H.P. (2006) mini-Tn7 insertion in bacteria with single *att*Tn7 sites: Example *Pseudomonas aeruginosa*. *Nat Protoc* **1**: 153–161.

Hanahan, D. (1983) Studies on transformation of *Escherichia coli* with plasmids. *J Mol Biol* **166**: 557–580.

Hogenkamp, F., Hilgers, F., Knapp, A., Klaus, O., Bier, C., Binder, D., et al. (2021) Effect of photocaged isopropyl-β-D-1-thiogalactopyranoside solubility on the light responsiveness of LacI-controlled expression systems in different bacteria. *ChemBioChem* **22**: 539–547.

Pascual, J., Lucena, T., Ruvira, M.A., Giordano, A., Gambacorta, A., Garay, E., et al. (2012) *Pseudomonas litoralis* sp. nov., isolated from mediterranean seawater. *Int J Syst Evol Microbiol* **62**: 438–444.

Penfold, R.J. and Pemberton, J.M. (1992) An improved suicide vector for construction of chromosomal insertion mutations in bacteria. *Gene* **118**: 145–146.

Prior, J.E., Lynch, M.D., and Gill, R.T. (2010) Broad-host-range vectors for protein expression across Gram negative hosts. *Biotechnol Bioeng* **106**: 326–332.

Sambrook, J., Fritsch, E., and Maniatis, T. (1989) Molecular Cloning: A Laboratory manual, 4th Edition. Cold Spring Harbor Laboratory Press.

Sánchez, D., Mulet, M., Rodríguez, A.C., David, Z., Lalucat, J., and García-Valdés, E. (2014) *Pseudomonas aestusnigri* sp. nov., isolated from crude oil-contaminated intertidal sand samples after the prestige oil spill. *Syst Appl Microbiol* **37**: 89–94.

Simon, R., Priefer, U., and Puhl, A. (1983) A broad host range mobilization system for *in vivo* genetic engineering: transposon mutagenesis in Gram negative bacteria. *Nat Biotechnol* **1**: 784–791.

Verhoef, S., Ballerstedt, H., Volkers, R.J.M., De Winde, J.H., and Ruijssenaars, H.J. (2010) Comparative transcriptomics and proteomics of p-hydroxybenzoate producing *Pseudomonas putida* S12: Novel responses and implications for strain improvement. *Appl Microbiol Biotechnol* **87**: 679–690.

Wang, M.Q. and Sun, L. (2016) *Pseudomonas oceani* sp. nov., isolated from deep seawater. *Int J Syst Evol Microbiol* **66**: 4250–4255.

Weihmann, R., Kubicki, S., Bitzenhofer, N.L., Domröse, A., Bator, I., Kirschen, L.-M., et al. (2023) The modular pYT vector series employed for chromosomal gene integration and expression to produce carbazoles and glycolipids in *P. putida*. *FEMS Microbes* **4**: 1–17.

Zhang, D.C., Liu, H.C., Zhou, Y.G., Schinner, F., and Margesin, R. (2011) *Pseudomonas bauzanensis* sp. nov., isolated from soil. *Int J Syst Evol Microbiol* **61**: 2333–2337.

Zobel, S., Benedetti, I., Eisenbach, L., De Lorenzo, V., Wierckx, N., and Blank, L.M. (2015) Tn7-Based Device for Calibrated Heterologous Gene Expression in Pseudomonas putida. *ACS Synth Biol* **4**: 1341–1351.